HHS Public Access

Author manuscript

ACS Catal. Author manuscript; available in PMC 2021 February 21.

Published in final edited form as:

ACS Catal. 2020 February 21; 10(4): 2791–2798. doi:10.1021/acscatal.9b05597.

Size-Controlled Chemoenzymatic Synthesis of Homogeneous Oligosaccharides of *Neisseria meningitidis* W Capsular Polysaccharide

Riyao Li[a], **Hai Yu**[a], **Saddam M. Muthana**[b], **Darón I. Freedberg**[c], **Xi Chen**[a,*]

[a]Department of Chemistry, University of California, One Shields Avenue, Davis, California 95616, United States

[b]Department of Chemistry, Alfaisal University, Riyadh, 11533, Kingdom of Saudi Arabia

[c]Laboratory of Bacterial Polysaccharides, Food and Drug Administration (FDA), Silver Spring, MD 20993, United States

Abstract

Neisseria meningitidis (Nm) serogroup W (NmW) is one of the six meningococcal serogroups that cause majority of invasive meningococcal diseases (IMD). Its capsular polysaccharide (CPS) is a virulence factor and is a key component in NmW CPS-protein conjugate vaccines. The current clinically used NmW CPS-protein conjugate vaccines are effective but the costs are high and the products are heterogeneous at both the CPS and the conjugate levels. Towards the development of potentially better NmW CPS vaccines, herein we report the synthesis of homogeneous oligosaccharides of NmW CPS in a size-controlled manner using polysaccharide synthase $NmSiaD_W$ in a sequential one-pot multienzyme (OPME) platform. Taking advantage of the obtained structurally defined synthetic oligosaccharides tagged with a hydrophobic chromophore, detailed biochemical characterization of $NmSiaD_W$ has been achieved. While the catalytic efficiency of the galactosyltransferase activity of $NmSiaD_W$ increases dramatically with the increase of the sialoside acceptor substrate size, the size difference of the galactoside acceptor substrate does not influence $NmSiaD_W$ sialyltransferase activity significantly. The ratio of donor and acceptor substrate concentrations, but not the size of the acceptor substrates, has been found to be the major determining factor for the sizes of the oligosaccharides produced. NmW CPS oligosaccharides with a degree of polymerization (DP) higher than 65 have been observed. The study provides a better understanding of $NmSiaD_W$ capsular polysaccharide synthase and showcases an efficient chemoenzymatic synthetic platform for obtaining structurally defined NmW CPS oligosaccharides in a size-controlled manner.

Graphical Abstract

*Corresponding Author: xiichen@ucdavis.edu.

Supporting Information.

This material is available free of charge via the Internet at http://pubs.acs.org.

$NmSiaD_W$ cloning, expression, biochemical characterization; detailed synthetic procedures, nuclear magnetic resonance (NMR) spectroscopy and high-resolution mass spectrometry (HRMS) data, and NMR spectra of products (PDF)

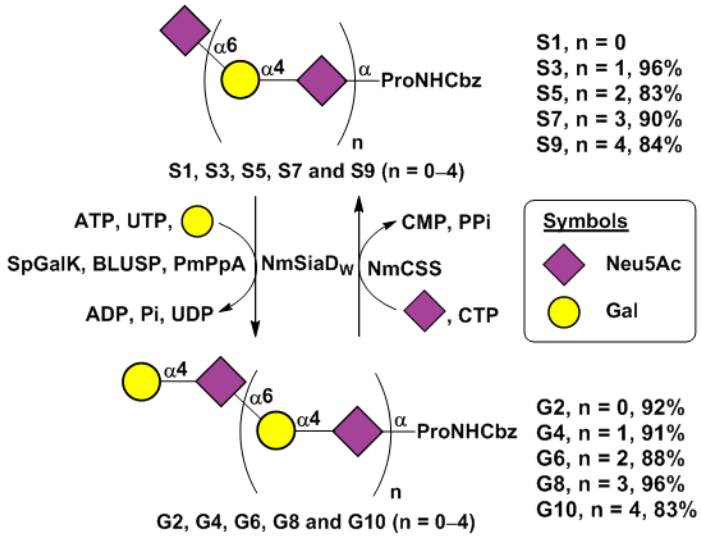

Keywords

biocatalysis; capsular polysaccharide; chemoenzymatic synthesis; *N. meningitidis* W; polysaccharide vaccine

Neisseria meningitidis (Nm) is a Gram-negative bacterium and a major cause of meningitis and septicemia.[1] Based on the structures of their capsular polysaccharides (CPSs), at least 12 Nm serogroups have been characterized.[2–3] Among them, six (Men A, B, C, W, X, and Y) are major causative agents of life-threatening invasive meningococcal diseases (IMDs).[4–6] Except for serogroup X (MenX), vaccines are currently available for the other five of these six Nm serogroups.[1] While meningococcal serogroup B (MenB) is prevented by meningococcal outer membrane protein vaccines such as MenB-FHbp and MenB-4C,[7] protection against infections caused by the other four serogroups relies mainly on capsular polysaccharide-protein conjugate vaccines where diphtheria protein cross-reactive materials 197 (CRM_{197}), diphtheria toxoid (D), or tetanus toxoid (TT) is used as the protein carrier.[1, 8] Among these, except for low-cost PsA-TT developed as an affordable meningococcal serogroup A (MenA) conjugate vaccine for meningitis belt countries,[9–10] the cost for the production of other conjugate vaccines is still high.[11] In addition, the current production of these conjugated vaccines involves extraction and purification of heterogeneous polysaccharides from bacterial cultures[12] followed by chemical derivatization and conjugation with a protein carrier.[13–14] Heterogeneity can be introduced at every step of this production process which may cause potential challenges in quality control. Undesired modification introduced may also led to complications.[15] Developing efficient methods for synthesizing structurally defined Nm CPSs could result in improved vaccine candidates with easier characterization, higher batch to batch reproducibility, higher efficiency, and potentially lower cost similar to the case of synthetic *Haemophilus influenza* type b (Hib) CPS conjugate vaccine.[15–16] Structurally defined oligosaccharides of Nm CPSs are also essential probes for better understanding the important roles of these biomolecules.[17–18]

In recent years, cases of invasive meningococcal diseases (IMD) caused by NmW have seen a sharp increase in numerous countries including England, the Netherlands, Australia, Canada, Argentina, Chile.[1] The CPS of NmW is a heteropolymer containing *N*-acetylneuraminic acid (Neu5Ac) and galactose (Gal) in a unique disaccharide repeating unit −4Neu5Acα2–6Galα1- that has not been found in other organisms.[3, 19–20] *N*-Acetylneuraminic acid (Neu5Ac) is the most common form of sialic acid (Sia), a family of more than 50 different structures containing a nine-carbon α-keto acid backbone.[21] The Neu5Ac in the CPS of NmW can be modified by *O*-acetylation at C-7 and/or C-9 in some NmW isolates.[22] Although still debatable, such *O*-acetyl modifications does not seem to affect the efficacy of NmW conjugate vaccines significantly.[12]

Chemical synthesis of NmW CPS oligosaccharides containing Neu5Ac at the non-reducing end ranging from disaccharide to decasaccharide has been accomplished with numerous protection and deprotection processes and the products have been used as valuable probes and vaccine candidates.[23] To the best of our knowledge, size-defined NmW CPS oligosaccharides containing Gal at the non-reducing end have not been produced. Towards the goal of producing better quality synthetic CPS conjugate vaccines, we have successfully developed an efficient chemoenzymatic method for synthesizing homogeneous oligosaccharides of NmW CPS in a size-controlled manner.

The key enzyme for the biosynthesis of NmW CPS is a polymerase $NmSiaD_W$ that has both α1–4-galactosyltransferase (α1–4GalT) and α2–6-sialyltransferase (α2–6SiaT) activities.[3, 20] While its N-terminal hexosyltransferase domain shares protein sequence homology with other Carbohydrate Active enZyme (CAZy) database[24–26] GT4 family glycosyltransferases,[20] its C-terminal sialyltransferase domain in a new CAZy GT97 family does not have significant protein sequence similarity with other known sialyltransferases except for homologs in NmY strains.[27] The dual glycosyltransferase activities of recombinant $NmSiaD_W$ have been confirmed by radioactivity assays using CPS isolated from NmW, its partially hydrolyzed products, and an α2–8-linked trisialoside as primers.[3] A P310G mutation in the N-terminal hexosyltransferase domain of $NmSiaD_W$ alters its activity preference from an α1–4-galactosyltransferase to an α1–4-glucosyltransferase for the formation of NmY CPS.[3, 20] However, detailed kinetics data of $NmSiaD_W$ are not currently available.

To obtain $NmSiaD_W$, its synthetic gene optimized for *E. coli* expression was cloned into pET22b (+) vector and $NmSiaD_W$ was expressed as a C-terminal His_6-tagged protein in *Escherichia coli* BL21 (DE3). About 150 mg soluble and active enzyme per liter of cell culture was routinely obtained after one-step purification with a nickel-nitrilotriacetic acid (Ni^{2+}-NTA) affinity column (Figure S1). It was important to add a detergent such as 0.1% Triton X-100 in the lysis buffer to obtain optimal amounts of $NmSiaD_W$ in a soluble form, indicating the association of the enzyme with membrane.

To facilitate enzyme characterization and product purification, a chromophore (Cbz)-tagged sialylmonosaccharide substrate was designed. Sialylmonosaccharide (**S1**) 2-*O*-(*N*-benzyloxycarbonyl)aminopropyl α-*N*-acetylneuraminide (Neu5AcαProNHCbz) was chemically synthesized from Neu5Ac (Scheme 1) similarly to that reported previously.[28]

Briefly, methylation of the carboxyl group in the commercially available Neu5Ac (**1**) followed by peracetylation produced per-*O*-acetylated Neu5Ac methyl ester (**3**) in 86% yield. Treatment of 3 with acetyl chloride in dichloromethane and anhydrous methanol formed per-*O*-acetylated Neu5Ac chloride (**4**), which was reacted with benzyl *N*-(3-hydroxypropyl) carbamate in the presence of AgOTf to produce protected Neu5Ac glycoside (**5**) in an excellent 91% yield. De-*O*-acetylation using NaOMe in MeOH and hydrolysis of methyl ester using sodium hydroxide produced the desired product Neu5Acα*ProNHCbz (**S1**, 3.79 g) in 84% yield.

Using **S1** as the acceptor substrate, the α1–4-galactosyltransferase activity of $NmSiaD_W$ was shown to be active in a broad pH range of 5.0–9.5 and optimal activities were observed at pH 6.5 and pH 9.0. In comparison, using galactosyldisaccharide **G2** (see below and Scheme 2) as the acceptor substrate, the α2–6-sialyltransferase activity of $NmSiaD_W$ was shown to be active in a pH range of 6.0–9.5 with an optimum at pH 8.0 (Figure S2). The addition of a metal ion such as Mn^{2+}, Mg^{2+}, Co^{2+}, Na^{+}, Ca^{2+}, Li^{+}, Ni^{2+} was not required and did not significantly affect either glycosyltransferase activities of $NmSiaD_W$ although the addition of Cu^{2+} completely abolished both activities (Figure S3). The α1–4-galactosyltransferase domain of $NmSiaD_W$ seemed to be more stable than its α2–6-sialyltransferase domain. The activity of the former retained after being incubated for 30 minutes at a temperature up to 33 °C, while the activity of the latter decreased significantly after incubation for 30 minutes at a temperature higher than 30 °C (Figure S4). Both glycosyltransferase activities were lost when $NmSiaD_W$ was incubated at 44 °C for 30 minutes. The optimal temperature for the α1–4-galactosyltransferase activity was in a broad range of 20–33 °C, while the optimal sialyltransferase activity had a narrower range of 30–37 °C (Figure S5).

Knowing the optimal conditions of both glycosyltransferase activities of $NmSiaD_W$, NmW CPS oligosaccharides ranging from galactosyldisaccharide **G2** to galactosyldecasaccharide **G10** were synthesized from sialylmonosaccharide Neu5Acα*ProNHCbz (**S1**) using a sequential one-pot multienzyme (OPME) process. As shown in Scheme 2, an OPME α1–4-galactosylation system (**OPME1**) containing *Streptococcus pneumoniae* TIGR4 galactokinase (SpGalK),[29] *Bifidobacterium longum* UDP-sugar pyrophosphorylase (BLUSP),[30] *Pasteurella multocida* inorganic pyrophosphatase (PmPpA),[31] and $NmSiaD_W$ was used to add an α1–4-linked galactose residue to a sialoside acceptor such as **S1**. In this system, SpGalK was responsible for the formation of galactose-1-phosphate (Gal-1-P) which was used by BLUSP to form activated sugar nucleotide uridine-5'-diphosphate galactose (UDP-Gal), the donor substrate of the α1–4-galactosyltransferase activity of $NmSiaD_W$ for the synthesis of galactosides such as **G2**. PmPpA was included to hydrolyze the inorganic pyrophosphate (PPi) formed in the BLUSP-catalyzed reaction to drive the reaction towards the formation of UDP-Gal. From **S1**, galactosyldisaccharide **G2** (1.26 g) was synthesized and purified with an excellent 92% yield.

Subsequently, an OPME α2–6-sialylation system (**OPME2**) containing *Neisseria meningitidis* CMP-sialic acid synthetase (NmCSS)[32] and $NmSiaD_W$ was used to sialylate the galactoside formed. In this system, NmCSS catalyzed the formation of cytidine-5'-monophosphate Neu5Ac (CMP-Neu5Ac), the activated sugar nucleotide donor for the α2–6-sialyltransferase activity of $NmSiaD_W$ for the synthesis of α2–6-linked sialosides such as **S3**

(Scheme 2). From **G2**, sialyltrisaccharide **S3** (620 mg) was synthesized and purified with an excellent 96% yield.

Repeating the OPME α1–4-galactosylation and OPME α2–6-sialylation reactions sequentially with product purification after each OPME reaction to provide the acceptor substrate for the next OPME reaction led to the efficient synthesis of a series of NmW CPS oligosaccharides in 83–96% yields including **G4** (556 mg, 91%), **S5** (512 mg, 83%), G6 (440 mg, 88%), **S7** (418 mg, 90%), **G8** (380 mg, 96%), **S9** (301 mg, 84%), and **G10** (221 mg, 83%).

These reactions were carried out in 0.25–1.00 g scales in Tris-HCl buffer (100 mM, *p*H 8.5) containing $MgCl_2$ (20 mM) with the consideration of acceptable and optimal reaction conditions of $NmSiaD_W$ and other enzymes involved in the sequential OPME reactions. Except for the synthesis of galactosyldisaccharide **G2** from sialylmonosaccharide **S1** which required a long reaction time (98 h), all other OPME reactions were carried out at 30 °C for 20 h. Assisted by the Cbz-tag, product purification was conveniently achieved by passing the reaction mixture through a C18 reverse phase column twice. The first column purification used a gradient solution of 0.1% trifluoroacetic acid (TFA) in H_2O and acetonitrile as an eluent to separate the protonated product from other components in the reaction mixture. The fractions containing the product were neutralized by NaOH immediately to minimize acid-catalyzed hydrolysis. The second C18 column purification used a gradient solution of water and acetonitrile to obtain the desired pure product whose structure and purity were confirmed by nuclear magnetic resonance (NMR), high resolution mass spectrometry (HRMS), and ultra-high performance liquid chromatography (UHPLC) (Figure S6) analyses. Heteronuclear Single Quantum Coherence-Total Correlation Spectroscopy (HSQC-TOCSY)[33–34] studies for **S1–G10** with 90 ms and 10 ms mixing times (**ESI**) clearly show independent coupling networks of terminal and internal Neu5Ac or Gal residues. For example, for **S3** which contains two Neu5Ac residues, the chemical shifts of the internal Neu5Ac are more downfield for $H3_{eq}$, H4, H5 H6 (0.05–0.20 ppm difference), and C4 (4.28 ppm difference) but more upfield for $H3_{ax}$ (0.09 ppm difference), C3 (3.32 ppm difference), and C5 (2.27 ppm difference) than those of the terminal Neu5Ac with no significant differences for C6 (Figure S7A–S7B). In comparison, for **G4** which contains two Gal residues, the chemical shifts of the protons on the Gal backbones (less than 0.05 ppm difference) and C1 (0.65 ppm difference) are slightly more upfield for the internal residue (Figure S7C).

The obtained Cbz-tagged monosaccharide and oligosaccharides of NmW CPS (**S1–G10**) were used as indispensable acceptor substrates for $NmSiaD_W$ kinetics studies by varying the concentrations of the acceptor with a fixed concentration of the donor (Figure S8). As shown in Table 1 and Table 2, two distinctive kinetics behaviors were observed for the two glycosyltransferase activities of $NmSiaD_W$.

Using sialosides **S1–S9** as acceptors, it was shown that the catalytic efficiency (k_{cat}/K_M) of $NmSiaD_W$ α1–4-galactosyltransferase activity increased significantly as the length of the acceptor substrate increased (Table 1). This was mainly due to the decrease of K_M from higher than 10.0 mM for **S1** to 0.89±0.10 mM for **S3**, 0.10±0.02 mM for **S5**, 0.07±0.01 mM

for **S7**, and less than 0.05 mM for **S9**. Remarkably, the overall catalytic efficiency increased by more than 2100-fold with sialylnonasaccharide **S9** acceptor compared to that with sialylmonosaccharide **S1** acceptor. Acceptor substrate inhibition was observed when the concentration of **S9** was higher than 2 mM. This can be explained by the low K_M value of **S9** which may compete with the donor binding to the enzyme, inhibiting an effective catalytic process by glycosyltransferases which follows an ordered sequential Bi-Bi mechanism where the enzyme binds the sugar nucleotide before the acceptor.[35] On the other hand, the k_{cat} (5.1–8.8 s^{-1}) did not change significantly as the length of the sialoside acceptor varied. A similar preference for longer acceptor substrates was demonstrated previously for a GT4 family glucosyltransferase using lipid acceptors.[36]

In contrast to the kinetics properties of the α1–4-galactosyltransfearse activity of $NmSiaD_W$, using galactosides **G2–G10** as acceptors, the catalytic efficiency (k_{cat}/K_M) of $NmSiaD_W$ α2–6-sialyltransferase activity was shown to be in a narrow range of 46–97 s^{-1} mM^{-1} without significant change when the length of the acceptor substrate was varied (Table 2). The k_{cat} was in a range of 7.03–23.1 s^{-1} and the K_M fell in the range of 0.13–0.24 mM. When **G4** was used as the acceptor, $NmSiaD_W$ α2–6-sialyltransferase activity had the highest catalytic efficiency (97 s^{-1} mM^{-1}) compared to the other four acceptors (k_{cat}/K_M = 46–55 s^{-1} mM^{-1}) mainly due to a relatively higher k_{cat} (23.1 ±1.1 s^{-1}) than those of **G2**, **G6**, **G8**, and **G10** (7.03–11.9 s^{-1}).

$NmSiaD_W$ kinetics studies by varying the concentrations of the donors (Figure S9) were also investigated using a fix concentration of a representative short or long acceptor substrate. **S3** or **S9** was used as the acceptor substrate for varying the concentration of UDP-Gal and **G2** or **G10** was used as the acceptor substrate for varying the concentration of CMP-Neu5Ac. As shown below, the kinetics parameters for the α1–4-galactosyltransferase (Table 3) and the α2–6-sialyltransferase (Table 4) activities of $NmSiaD_W$ did not change significantly when different sizes of acceptors were used.

The availability of chromophore-tagged NmW CPS mono- and oligosaccharides with defined sizes and structures (**S1–G10**) allowed us to address several questions: 1, does the length of $NmSiaD_W$ oligosaccharide acceptor affect the maximal product sizes when both donors are provided? 2, does the identity of the monosaccharide at the reducing end of the oligosaccharide acceptor affect the maximal product sizes? and 3, what is the effect of the donor versus acceptor ratio on the product size distribution?

To answer the first two questions, $NmSiaD_W$-catalyzed polymerization reactions were carried out with an acceptor (5 mM) selected from **S1–G10** and 10 equivalents of both UDP-Gal and CMP-Neu5Ac donors. Reaction mixtures were analyzed using an UHPLC system with an AdvanceBio Glycan Mapping column (a HILIC column) using NaCl and acetonitrile gradients. As shown in Figure S10, except for the reactions using **S1** as the acceptor which were slow, no significant difference on the maximal product sizes was observed when oligosaccharide acceptors (**G2–G10**) of different sizes were used. Nevertheless, compared to reactions with a shorter acceptor (**G2–S7**), a narrower product size distribution was seen for reactions with a longer oligosaccharide acceptor (**G8**, **S9**, or **G10**). Therefore, using longer oligosaccharide acceptors (G8–G10) could be advantages for the production of

monodisperse NmW capsular polysaccharides. The identity of the reducing-end monosaccharide did not seem to affect the maximal product sizes either. It was interesting to observe (in Figure S10 and also in Figure 1 below) that sialosides seemed to be the preferred products when a sialoside was used as the starting acceptor substrate. In comparison, a galactoside starting acceptor led to the formation of both galactoside and sialoside products. The underlying reason is unclear but could be related to the difference in the relative availability of two donor substrates in the reaction mixtures. Polysaccharides with a degree of polymerization (DP) for up to 33 were observed in 20 h reactions. The most abundant products had a DP distribution in the range of DP17–23.

The effect of the donor verses acceptor ratio on the product size distribution was investigated using a series of ratios varying from 1 to 50 with either **G2** or **S3** as the acceptor. As shown in Figure 1 and Figure S11, the sizes of the products increased with the increase of the donor versus acceptor ratio independent of whether a galactoside **G2** or a sialoside **S3** was used as the acceptor. Polymers with DP59 or higher were observed. In comparison, $NmSiaD_W$ was reported to form products for up to DP19 using Neu5Acα2–6Galα1–4Neu5AcαMU as the acceptor and 4 equivalents of both donors.[27] The strategy of using a high donor versus acceptor ratio was also applied previously for synthesizing monodisperse polysaccharides such as hyaluronan (up to 8 MDa) using *Pasteurella multocida* hyaluronan synthase (PmHAS)[37] and heparosan (800 kDa) using *Pasteurella multocida* heparosan synthase 1 (PmHS1).[38]

Assuming oligosaccharides **S3–G8** were not part of the products in the 20-h reactions using 50 equivalents of donors (Figure 1 and Figure S11), more detailed analyses showed that when G2 was used as the acceptor substrate, the average molecular weights (M_n or M_w) of $NmSiaD_W$ products increased from 1.0 kDa to 6.1–6.6 kDa when the donor versus acceptor ratio changed from 1 to 50 (Table S1) and the product average molecular weights increased from 1.4 kDa to 7.5–8.6 kDa when **S3** was used as the acceptor substrate (Table S2). $NmSiaD_W$ catalyzed the formation of low molecular weight polysaccharides with a narrow size distribution (polydispersity index: M_w/M_n = 1.03–1.14) under the experimental conditions used.

The application of *in situ* generation of sugar nucleotide donors (UDP-Gal and CMP-Neu5Ac) by OPME galactosylation and sialylation systems in polymerization reaction was investigated using **G2** or **S3** as the acceptor substrate and compared to the reactions using 10 equivalents of donor substrates. The OPME polymerization reactions were carried out in two steps where the sugar nucleotides were formed at 30 °C for 10 hours in Tris-HCl buffer from ATP, UTP, Gal, CTP, Neu5Ac at pH 8.5 in the presence of SpGalK, BLUSP, PmPpA, and NmCSS. The reaction mixture was then added with **G2** or **S3**, and $NmSiaD_W$ for polymerization reactions. As shown in Figure S12, polymerization reactions with OPME systems were slower but reached similar levels as those using sugar nucleotides as starting materials in a 20-h reaction time.

In conclusion, a sequential OPME platform has been successfully established for efficient synthesis of homogeneous NmW CPS oligosaccharides in a size-controlled manner. The hydrophobic chromophore (Cbz) tag in the starting acceptor substrate facilitates not only the

product purification but also the application of the products in detailed biochemical characterization of the polymerase $NmSiaD_W$. While the binding affinity and the catalytic efficiency of the α1–4-galactosyltransferase activity of $NmSiaD_W$ increased dramatically with the increase of the size of the sialoside acceptors, the corresponding parameters for the α2–6-sialyltransferase activity of $NmSiaD_W$ do not change significantly with the increase of the galactoside acceptor size. The oligosaccharide product sizes of $NmSiaD_W$–catalyzed polymerization reactions are influenced significantly by the ratio of donor and acceptor concentrations but less by the size of the oligosaccharide acceptors used. The structurally defined NmW CPS oligosaccharides synthesized are valuable probes and carbohydrate standards. They are also candidates for developing better bacterial carbohydrate-protein conjugate vaccines. The sequential OPME strategy can be extended for chemoenzymatic synthesis of other polysaccharides containing disaccharide repeating units.

Supplementary Material

Refer to Web version on PubMed Central for supplementary material.

ACKNOWLEDGMENT

This work was supported by the United States National Institutes of Health (NIH) Common Fund for Glycoscience Program grant U01GM125288. The Bruker Avance-800 NMR spectrometer was funded by the United States National Science Foundation grant DBIO-722538. We would like to thank Prof. Enoch Baldwin at UC Davis for helpful discussion related to $NmSiaD_W$ kinetics studies and Wanqing Li and Dr. Ping Yu at UC Davis for providing help for HSQC-TOCSY NMR characterization.

REFERENCES

(1). Presa J; Findlow J; Vojicic J; Williams S; Serra L Epidemiologic Trends, Global Shifts in Meningococcal Vaccination Guidelines, and Data Supporting the Use of MenACWY-TT Vaccine: A Review. Infect. Dis. Ther. 2019, 8, 307–333. [PubMed: 31347097]

(2). Tsang RS; Tsai CM; Henderson AM; Tyler S; Law DK; Zollinger W; Jamieson F Immunochemical Studies And Genetic Background of Two *Neisseria meningitidis* Isolates Expressing Unusual Capsule Polysaccharide Antigens With Specificities of Both Serogroup Y And W135. Can. J. Microbiol. 2008, 54, 229–234. [PubMed: 18388994]

(3). Romanow A; Haselhorst T; Stummeyer K; Claus H; Bethe A; Muhlenhoff M; Vogel U; von Itzstein M; Gerardy-Schahn R Biochemical and Biophysical Characterization of The Sialyl-/Hexosyltransferase Synthesizing The Meningococcal Serogroup W135 Heteropolysaccharide Capsule. J. Biol. Chem. 2013, 288, 11718–11730. [PubMed: 23439648]

(4). Acevedo R; Bai X; Borrow R; Caugant DA; Carlos J; Ceyhan M; Christensen H; Climent Y; De Wals P; Dinleyici EC; Echaniz-Aviles G; Hakawi A; Kamiya H; Karachaliou A; Lucidarme J; Meiring S; Mironov K; Safadi MAP; Shao Z; Smith V; Steffen R; Stenmark B; Taha MK; Trotter C; Vazquez JA; Zhu B The Global Meningococcal Initiative Meeting on Prevention of Meningococcal Disease Worldwide: Epidemiology, Surveillance, Hypervirulent Strains, Antibiotic Resistance And High-Risk Populations. Expert Rev. Vaccines 2019, 18, 15–30. [PubMed: 30526162]

(5). Batista RS; Gomes AP; Dutra Gazineo JL; Balbino Miguel PS; Santana LA; Oliveira L; Geller M Meningococcal Disease, A Clinical And Epidemiological Review. Asian Pac. J. Trop. Med. 2017, 10, 1019–1029. [PubMed: 29203096]

(6). Rouphael NG; Stephens DS Neisseria meningitidis: Biology, Microbiology, And Epidemiology. Methods Mol. Biol. 2012, 799, 1–20. [PubMed: 21993636]

(7). McNamara LA; Thomas JD; MacNeil J; Chang HY; Day M; Fisher E; Martin S; Poissant T; Schmink SE; Steward-Clark E; Jenkins LT; Wang X; Acosta A; Oregon Meningococcal Carriage

T Meningococcal Carriage Following A Vaccination Campaign With MenB-4C and MenB-FHbp in Response to a University Serogroup B Meningococcal Disease Outbreak-Oregon, 2015–2016. J. Infect. Dis. 2017, 216, 1130–1140. [PubMed: 28968661]

(8). Pichichero ME Protein Carriers of Conjugate Vaccines: Characteristics, Development, And Clinical Trials. Hum. Vaccines Immunother. 2013, 9, 2505–2523.

(9). LaForce FM; Djingarey M; Viviani S; Preziosi MP Lessons From The Meningitis Vaccine Project. Viral Immunol. 2018, 31, 109–113. [PubMed: 29116892]

(10). Tiffay K; Jodar L; Kieny MP; Socquet M; LaForce FM The Evolution of The Meningitis Vaccine Project. Clin. Infect. Dis. 2015, 61 Suppl 5, S396–S403. [PubMed: 26553666]

(11). Vella M; Pace D Glycoconjugate Vaccines: An Update. Expert Opin. Biol. Ther. 2015, 15, 529–546. [PubMed: 25496172]

(12). Berti F; De Ricco R; Rappuoli R Role of O-Acetylation in The Immunogenicity of Bacterial Polysaccharide Vaccines. Molecules. 2018, 23, 1340.

(13). Lee CH; Kuo WC; Beri S; Kapre S; Joshi JS; Bouveret N; LaForce FM; Frasch CE Preparation And Characterization of An Immunogenic Meningococcal Group A Conjugate Vaccine For Use in Africa. Vaccine. 2009, 27, 726–732. [PubMed: 19063929]

(14). Berti F; Adamo R Antimicrobial Glycoconjugate Vaccines: An Overview of Classic And Modern Approaches For Protein Modification. Chem. Soc. Rev. 2018, 47, 9015–9025. [PubMed: 30277489]

(15). Kaplonek P; Khan N; Reppe K; Schumann B; Emmadi M; Lisboa MP; Xu F-F; Calow ADJ; Parameswarappa SG; Witzenrath M; Pereira CL; Seeberger PH Improving Vaccines Against *Streptococcus pneumoniae* Using Synthetic Glycans. Proc. Natl. Acad. Sci. U. S. A. 2018, 115, 13353–13358. [PubMed: 30530654]

(16). Verez-Bencomo VF-S,V; Hardy E; Toledo ME; Rodríguez MC; Heynngnezz L; Rodriguez A; Baly A; Herrera L; Izquierdo M; Villar A; Valdés Y; Cosme K; Deler ML; Montane M; Garcia E; Ramos A; Aguilar A; Medina E; Toraño G; Sosa I; Hernandez I; Martínez R; Muzachio A; Carmenates A; Costa L; Cardoso F; Campa C; Diaz M; Roy R A Synthetic Conjugate Polysaccharide Vaccine Against *Haemophilus influenzae* Type b. Science 2004, 305, 522–525. [PubMed: 15273395]

(17). Geissner A; Reinhardt A; Rademacher C; Johannssen T; Monteiro J; Lepenies B; Thepaut M; Fieschi F; Mrazkova J; Wimmerova M; Schuhmacher F; Gotze S; Grunstein D; Guo X; Hahm HS; Kandasamy J; Leonori D; Martin CE; Parameswarappa SG; Pasari S; Schlegel MK; Tanaka H; Xiao G; Yang Y; Pereira CL; Anish C; Seeberger PH Microbe-Focused Glycan Array Screening Platform. Proc. Natl. Acad. Sci. U. S. A. 2019, 116, 1958–1967. [PubMed: 30670663]

(18). Purohit S; Li T; Guan W; Song X; Song J; Tian Y; Li L; Sharma A; Dun B; Mysona D; Ghamande S; Rungruang B; Cummings RD; Wang PG; She JX Multiplex Glycan Bead Array For High Throughput And High Content Analyses of Glycan Binding Proteins. Nat. Commun. 2018, 9, 258–269. [PubMed: 29343722]

(19). Bhattacharjee AK; Jennings HJ; Kenny CP; Martin A; Smith IC Structural Determination of The Polysaccharide Antigens of *Neisseria meningitidis* Serogroups Y, W-135, and BO1. Can. J. Biochem. 1976, 54, 1–8. [PubMed: 814976]

(20). Claus H; Stummeyer K; Batzilla J; Muhlenhoff M; Vogel U Amino Acid 310 Determines The Donor Substrate Specificity of Serogroup W-135 And Y Capsule Polymerases of *Neisseria meningitidis*. Mol. Microbiol. 2009, 71, 960–971. [PubMed: 19170877]

(21). Chen X; Varki A Advances in The Biology And Chemistry of Sialic Acids. ACS Chem. Biol. 2010, 5, 163–176. [PubMed: 20020717]

(22). Claus H; Borrow R; Achtman M; Morelli G; Kantelberg C; Longworth E; Frosch M; Vogel U Genetics of Capsule *O*-Acetylation in Serogroup C, W-135 And Y Meningococci. Mol. Microbiol. 2004, 51, 227–239. [PubMed: 14651624]

(23). Wang CH; Li ST; Lin TL; Cheng YY; Sun TH; Wang JT; Cheng TJ; Mong KK; Wong CH; Wu CY Synthesis of *Neisseria meningitidis* Serogroup W135 Capsular Oligosaccharides For Immunogenicity Comparison And Vaccine Development. Angew. Chem. Int. Ed. Engl. 2013, 52, 9157–9161. [PubMed: 23843313]

(24). Campbell JA; Davies GJ; Bulone V; Henrissat B A Classification of Nucleotide-Diphospho-Sugar Glycosyltransferases Based on Amino Acid Sequence Similarities. Biochem. J. 1997, 326 (Pt 3), 929–939. [PubMed: 9334165]

(25). Coutinho PM; Deleury E; Davies GJ; Henrissat B An Evolving Hierarchical Family Classification for Glycosyltransferases. J. Mol. Biol. 2003, 328, 307–317. [PubMed: 12691742]

(26). Lombard V; Golaconda Ramulu H; Drula E; Coutinho PM; Henrissat B The Carbohydrate-Active Enzymes Database (CAZy) in 2013. Nucleic Acids Res. 2014, 42, D490–495. [PubMed: 24270786]

(27). Romanow A; Keys TG; Stummeyer K; Freiberger F; Henrissat B; Gerardy-Schahn R Dissection of Hexosyl- And Sialyltransferase Domains in The Bifunctional Capsule Polymerases from *Neisseria meningitidis* W And Y Defines A New Sialyltransferase Family. J. Biol. Chem. 2014, 289, 33945–33957. [PubMed: 25342753]

(28). Sardzik R; Sharma R; Kaloo S; Voglmeir J; Crocker PR; Flitsch SL Chemoenzymatic Synthesis of Sialooligosaccharides on Arrays for Studies of Cell Surface Adhesion. Chem. Commun. 2011, 47, 5425–5427.

(29). Chen M; Chen LL; Zou Y; Xue M; Liang M; Jin L; Guan WY; Shen J; Wang W; Wang L; Liu J; Wang PG Wide Sugar Substrate Specificity of Galactokinase From *Streptococcus pneumoniae* TIGR4. Carbohydr. Res. 2011, 346, 2421–2425. [PubMed: 21903203]

(30). Muthana MM; Qu J; Li Y; Zhang L; Yu H; Ding L; Malekan H; Chen X Efficient One-Pot Multienzyme Synthesis of UDP-Sugars Using A Promiscuous UDP-Sugar Pyrophosphorylase From Bifidobacterium longum (BLUSP). Chem. Commun. 2012, 48, 2728–2730.

(31). Lau K; Thon V; Yu H; Ding L; Chen Y; Muthana MM; Wong D; Huang R; Chen X Highly Efficient Chemoenzymatic Synthesis of beta1–4-Linked Galactosides with Promiscuous Bacterial beta1–4-Balactosyltransferases. Chem. Commun. 2010, 46, 6066–6068.

(32). Yu H; Yu H; Karpel R; Chen X Chemoenzymatic Synthesis of CMP-Sialic Acid Derivatives by A One-Pot Two-Enzyme System: Comparison of Substrate Flexibility of Three Microbial CMP-Sialic Acid Synthetases. Bioorg. Med. Chem. 2004, 12, 6427–6435. [PubMed: 15556760]

(33). Lerner L; Bax A Sensitivity-Enhanced Two-Dimensional Heteronuclear Relayed Coherence Transfer NMR Spectroscopy. J. Magn. Reson. 1986, 69, 375–380.

(34). Lerner L; Bax A Application of New, High-Sensitivity, ^{1}H-^{13}C-N.M.R.-Spectral Techniques to The Study of Oligosaccharides. Carbohydr. Res. 1987, 166, 35–46. [PubMed: 3652076]

(35). Boix E; Zhang Y; Swaminathan GJ; Brew K; Acharya KR Structural Basis of Ordered Binding of Donor and Acceptor Substrates to The Retaining Glycosyltransferase, alpha-1,3-Galactosyltransferase. J. Biol. Chem. 2002, 277, 28310–28318. [PubMed: 12011052]

(36). Allison SE; D'Elia MA; Arar S; Monteiro MA; Brown ED Studies of The Genetics, Function, and Kinetic Mechanism of TagE, The Wall Teichoic Acid Glycosyltransferase in *Bacillus subtilis* 168. J. Biol. Chem. 2011, 286, 23708–23716. [PubMed: 21558268]

(37). Jing W; DeAngelis PL Synchronized Chemoenzymatic Synthesis of Monodisperse Hyaluronan Polymers. J. Biol. Chem. 2004, 279, 42345–42349. [PubMed: 15299014]

(38). Sismey-Ragatz AE; Green DE; Otto NJ; Rejzek M; Field RA; DeAngelis PL Chemoenzymatic Synthesis with Distinct Pasteurella Heparosan Synthases: Monodisperse Polymers and Unnatural Structures. J. Biol. Chem. 2007, 282, 28321–28327. [PubMed: 17627940]

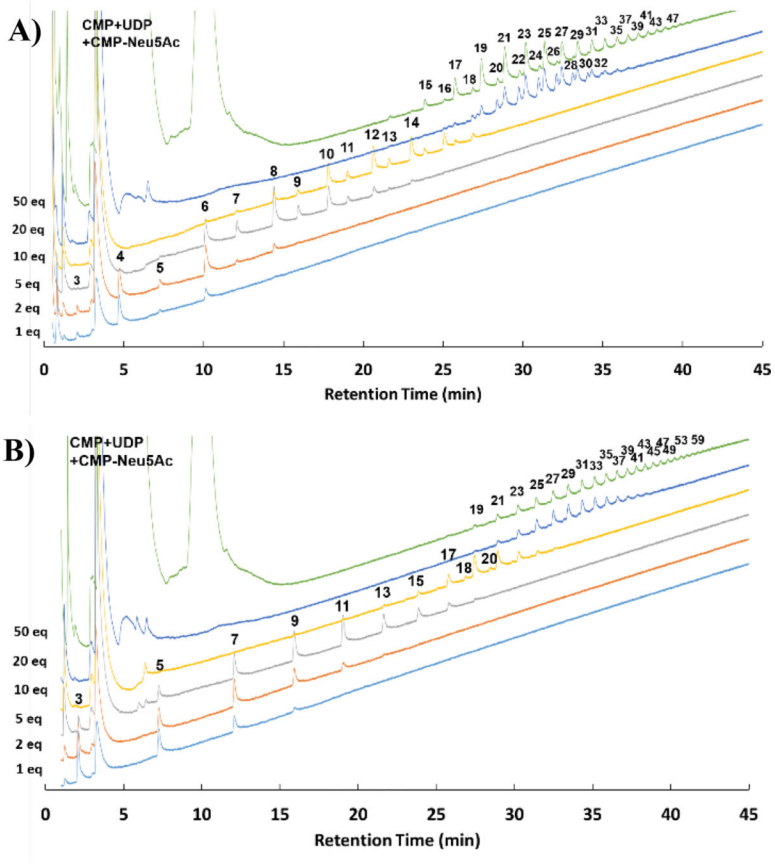

Figure 1.

Product profiles of 20-hour reactions using different ratios (1–50 equivalents) of donors versus acceptor (5 mM) where G2 (A) or S3 (B) was used as the acceptor.

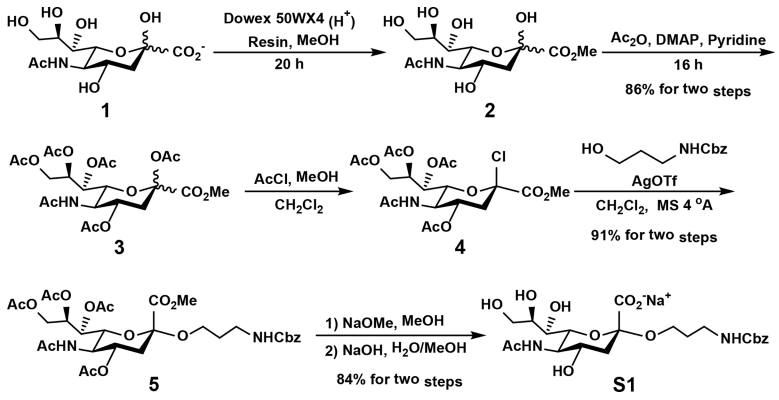

Scheme 1.

Chemical synthesis of sialylmonosaccharide S1 from *N*-acetylneuraminic acid (Neu5Ac, 1).

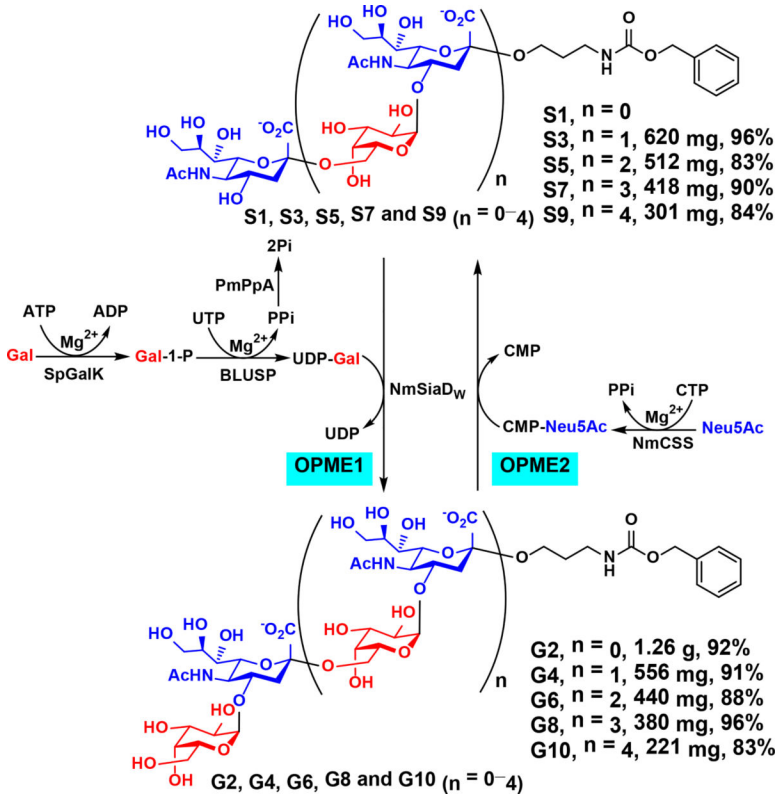

Scheme 2.

Sequential one-pot multienzyme (OPME) chemoenzymatic synthesis of oligosaccharides G2–G10 from monosaccharide S1.

Table 1.

Apparent kinetics data for $NmSiaD_W$ α1–4-galactosyltransferase activity using a fixed concentration of UDP-Gal. The averages of nonlinear regression standard errors from technical duplicates are shown.

Acceptor	k_{cat} (s^{-1})	K_M (mM)	k_{cat}/K_M (s^{-1} mM^{-1})
S1	/	>>10.0	4.7×10^{-2}
S3	8.8±0.4	0.89±0.10	10
S5	5.3±0.2	0.10±0.02	51
S7	5.5±0.2	0.07±0.01	83
S9	5.1±0.3	<0.05	$>1.0\times10^{2}$

Table 2.

Apparent kinetics data for $NmSiaD_W$ α2–6-sialyltransferase activity using a fixed concentration of CMP-Neu5Ac. The averages of nonlinear regression standard errors from technical duplicates are shown.

Acceptor	k_{cat} (s^{-1})	K_M (mM)	k_{cat}/K_M (s^{-1} mM^{-1})
G2	9.76±0.55	0.18±0.04	55
G4	23.1±1.1	0.24±0.04	97
G6	11.9±0.5	0.23±0.04	53
G8	10.3±0.5	0.25±0.04	46
G10	7.03±0.39	0.13±0.03	55

Table 3.

Apparent kinetics data for $NmSiaD_W$ α1–4-galactosyltransferase activity using a fixed concentration of acceptor (**S3** or **S9**). The averages of nonlinear regression standard errors from technical duplicates are shown.

Acceptor	k_{cat} (s^{-1})	K_M (mM)	k_{cat}/K_M (s^{-1} mM^{-1})
S3	6.3±0.2	0.12±0.02	53
S9	9.0±0.2	0.15±0.02	60

Table 4.

Apparent kinetics data for $NmSiaD_W$ α2–6-sialyltransferase activity using a fixed concentration of acceptor (**G2** or **G10**). The averages of nonlinear regression standard errors from technical duplicates are shown.

Acceptor	k_{cat} (s^{-1})	K_M (mM)	k_{cat}/K_M (s^{-1} mM^{-1})
G2	7.1±0.2	0.27±0.03	26
G10	6.1±0.2	0.38±0.05	16